Electronic Supplementary Information

Remarkable Substitution Influence on the Mechanochromism of Cyanostilbene Derivatives

He Zhao,[a] Yongtao Wang,*[a] Steven Harriangton, [b] Lei Ma,*[b] Shuzhi Hu,*[c] Xue Wu, [d] Huan Tang,[a] Mei Xue,[a] and Yubin Wang [a]

[a] School of Chemistry and Chemical Engineering , Engineering research center of materials-oriented chemical engineering of Xinjiang Bingtuan/Key Laboratory of materials-oriented chemical engineering of Xinjiang Uygur Autonomous Region, Shihezi University, Shihezi, Xinjiang 832003, P. R. China.

[b] Tianjin International Center of nanoparticles and nanosystem, Tianjin University, Tianjin, 300072, P. R. China.

[c] Key lab for fuel cell technology of Guangdong Province, Guangdong, School of Chemistry and Chemical Engineering, South China University of Technology, Guangzhou, 510640, P. R. China.

[d] Key Laboratory of Materials Modification by Laser, Ion and Electron Beams (Dalian University of Technology), Ministry of Education, Dalian 116024, China

Table of Contens

wavelength = 360 nm.

Fig. S29. (A) Emission spectra of 2b in THF and THF/water mixtures with varying water fractions (f_w) and kept at room temperature above 2 h. (B) Plots of fluorescence peak location and intensity *vs* f_w for 2b. Concentration = 20 μM; excitation wavelength = 360 nm.

Fig. S30. (A) Emission spectra of 2c in THF and THF/water mixtures with varying water fractions (f_w) and kept at room temperature above 2 h. (B) Plots of fluorescence peak location and intensity *vs* f_w for 2c. Concentration = 20 μM; excitation wavelength = 360 nm.

Fig. S31. (A) Emission spectra of 2d in THF and THF/water mixtures with varying water fractions (f_w) and kept at room temperature above 2 h. (B) Plots of fluorescence peak location and intensity *vs* f_w for 2d. Concentration = 20 μM; excitation wavelength = 360 nm.

Fig. S32. Emission maxima of 2e during the grinding-annealing cycles. As = as prepared sample, G = ground sample; An= Annealing sample (annealing at 60 ^oC for 10 min). The numbers after G or An represent cycle numbers.

Fig. S33. (A) Emission spectra of the as-prepared, ground and annealing 2a solids, (D) their XRD patterns and (B and C) their photographs taken under UV illumination.

Fig. S34. Emission maxima of 2a during the grinding-annealing cycles. As = as prepared sample, G = ground sample; An= Annealing sample (annealing at 60 ^oC for 10 min). The numbers after G or An represent cycle numbers.

Fig. S35. (A) Emission spectra of the as-prepared, ground and annealing 2d solids, (D) their XRD patterns and (B and C) their photographs taken under UV illumination.

Fig. S36. Emission maxima of 2d during the grinding-annealing cycles. As = as prepared sample, G = ground sample; An= Annealing sample (annealing at 60 ^oC for 10 min). The numbers after G or An represent cycle numbers.

Fig. S37. XRD patterns of the as-prepared and ground 2b (A) and 2c (B) solids.

Fig. S38. TGA and DSC (inset) thermograms of 2a (A) and 2b (B) recorded under nitrogen atmosphere at the heating rate of 10 $^oC\ min^{-1}$.

Experimental Section

Chemicals and instruments

All the reagents were obtained from commercial sources and used without further purification. The organic solvents were of analytical grade quality and all were dried by traditional methods. In general, all the intermediates and final compounds were purified by column chromatography on silica gel (200-300 mesh), and crystallization from analytical grade solvents. Reactions were monitored by using thin layer chromatography (TLC) (Qingdao Jiyida silica gel reagent factory GF254).

^{1}H NMR spectra was obtained with a Varian inova-400-MHz instrument using tetramethylsilane (TMS) as the internal standard. ^{13}C NMR spectra were recorded on a Varian inova-100-MHz spectrometer. ESI/MS spectra were obtained on a Waters GCT Premier. MALDI/HRMS was obtained on a UltrafleXtreme MALDI-TOF/TOF mass spectrometer (Bruker, Germany). A MaPada UV-3200PCS spectrophotometer was used to record absorption spectra. Fluorescence spectra was recorded on a Hitachi F-2500 and solution fluorescence quantum yield was estimated by using 9,10-diphenylanthracen as standard (Φ_F = 90% in cyclohexane). Solid-state efficiencies were determined using a FLS920 Fluorescence Lifetime and Steady State Spectroscopy with the excitation wavelength of 365 nm. The ground-state geometries were optimized using the density functional with B3LYP hybrid functional at the basis set level of 6-31G(d). All calculations were performed using the Gaussian 09 package. Single-crystal X-ray diffraction intensity data were collected on a Bruker–Nonices Smart Apex CCD diffractometer with graphite-monochromated Mo-Ka radiation. Processing of the intensity data was carried out using the SAINT and SADABS routines, and the structure and refinement were conducted using the SHELTL suite of X-ray programs (version 6.10). Glass transition temperature was determined by DSC measurements carried out using Netzsch Gerätebau GmbH R.O. Thermal stability was determined by thermogravimetric analyzer (TGA, Netzsch STA449F3) over a temperature range of 25-1000 ^{o}C at a heating rate of 10 ^{o}C min^{-1} under a nitrogen atmosphere. Powder XRD measurements were conducted on D8 Advance (Bruker) with Cu Kα radiation in the range $10^{o} < 2\theta < 90^{o}$. Digital photographs were taken by Canon 550D (Canon, Japan) digital cameras.

Synthesis

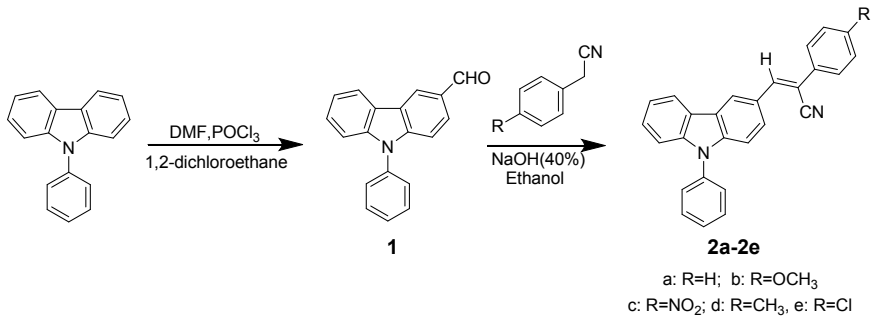

Scheme S1. Synthetic routes of target compounds 2a-2e.

Synthesis of 9-phenyl-9H-carbazole-3-carbaldehyde[1] (1)

The phosphorusoxychloride ($POCl_3$) was added dropwise to a stirred DMF solution at 0 °C. Then the temperature reached 20 °C, 1,2-dichloroethane solution of 9-phenyl-9H-carbazole was added dropwise to the stirred mixture solution. After the addition the mixture was refluxed with stirring for 7 h. The reaction was quenched by addition of ice water and extraction with CH_2Cl_2 (3×50 mL). The combined ethereal extracted was dried over anhydrous Na_2SO_4 and evaporated to dryness to leave a colorless residue, further purification by silica gel column chromatography (petroleum ether (PE) : ethyl acetate (EA) = 10:1, v/v) to give a white solid (yield 80%) : m.p. 100.5-100.6 °C.

2.2.2 Procedures for the synthesis of 2a-2e[2, 3]

(Z)-2-phenyl-3-(9-phenyl-9H-carbazol-3-yl)acrylonitrile (2a): A mixture of the 9-phenyl-9H-carbazole-3-carbaldehyde (7.38 mmol) and benzyl cyanide (7.38 mmol) was dissolved in 3 mL anhydrous ethanol. Then a 40% solution of sodium hydroxide (0.5 mL) was added into the reaction mixture. The mixture was stirred at room temperature for 12 h. After the reaction finished, the ice methanol was added dropwise to a stirred mixture solution. The pale yellow crystals formed was isolated by filtration and dried at 60 °C. Yield: 95%; m.p. 95.1-95.3 °C); ^{1}H NMR (DMSO-d_6, 400 MHz): δ (ppm) 8.84 (d, J = 1.6 Hz, 1H), 8.24 (d, J = 7.6 Hz, 1H), 8.20 (s, 1H), 8.12 (dd, J_1 = 8.8 Hz, J_2 = 2.0 Hz, 1H), 7.84-7.76 (m, 2H), 7.75-7.69 (m, 2H), 7.68-7.64 (m, 2H), 7.61-7.47 (m, 5H), 7.47-7.35 (m, 3H). ^{13}C NMR (DMSO-d_6, 400 MHz) δ (ppm) 144.07, 141.57, 141.30, 136.65, 134.76, 130.72, 129.62, 129.18, 128.58, 127.75, 127.50, 127.16, 126.36, 125.93, 123.38, 122.90, 122.87, 121.39, 120.95, 119.13, 110.61, 107.54. MS (ESI) *m/z* 371.2 $[M+H]^+$, HRMS (MALDI-TOF): *m/z* 370.1465 [M^+, calcd 370.1465].

(Z)-2-(4-methoxyphenyl)-3-(9-phenyl-9H-carbazol-3-yl)acrylonitrile (2b): Compound 2b was obtained from 2-(4-methoxyphenyl)acetonitrile and 1. Time: 10 h; yield: 98%; fluorescence yellow crystals; m.p. 157.4-157.6 °C; ^{1}H NMR (DMSO-d_6, 400 MHz): δ (ppm) 8.79 (s, 1H), 8.23 (d, J = 7.6 Hz, 1H), 8.12-8.02 (m, 2H), 7.76-7.63 (m, 6H),

7.61-7.45 (m, 3H), 7.43-7.34 (m, 2H), 7.05 (d, J = 8.8 Hz, 2H), 3.83 (s, 3H). ^{13}C NMR (DMSO-d_6, 400 MHz) δ (ppm) 160.16, 141.85, 141.32, 141.25, 136.70, 130.70, 128.52, 127.53, 127.42, 127.31, 127.14, 126.62, 123.36, 122.92, 122.45, 121.31, 120.92, 119.23, 115.02, 110.54, 107.40, 55.79. MS (ESI) *m/z* 423.3 $[M+Na]^+$, HRMS (MALDI-TOF): *m/z* 400.1561 [M^+, calcd 400.1570].

(Z)-2-(4-nitrophenyl)-3-(9-phenyl-9H-carbazol-3-yl)acrylonitrile (2c): Compound 2c was obtained from 2-(4-nitrophenyl)acetonitrile and 1. Time: 9 h; yield: 90%; orangered crystals; m.p. 200.7-200.9 °C; ^{1}H NMR (DMSO-d_6, 400 MHz): δ (ppm) 8.90 (s, 1H) 8.42 (s, 1H) 8.34 (d, J = 8.8 Hz, 2H) 8.23 (d, J = 7.6 Hz, 1H) 8.17 (d, J = 8.4 Hz, 1H) 8.05 (d, J = 8.8 Hz, 2H) 7.75-7.57 (m, 5H) 7.55-7.47 (m, 2H) 7.45-7.35 (m, 2H) ^{13}C NMR (DMSO-d_6, 400 MHz) δ (ppm) 147.01, 141.82, 141.12, 140.81, 136.15, 130.16, 128.16, 127.76, 126.70, 126.46, 125.39, 124.13, 123.08, 122.99, 122.44, 121.02, 120.36, 117.92, 110.21, 110.17, 105.03. MS (ESI) *m/z* 416.2 $[M+H]^+$, HRMS (MALDI-TOF): *m/z* 415.1316 [M^+, calcd 415.1315].

(Z)-3-(9-phenyl-9H-carbazol-3-yl)-2-(p-tolyl)acrylonitrile (2d): Compound 2d was obtained from 2-(p-tolyl)acetonitrile and 1. Time: 48 h Yield: 90%; pale yellow crystals; m.p. 173.5-173.8 °C; ^{1}H NMR ($CDCl_3$, 400 MHz): δ (ppm) 8.69 (d, J = 2.0 Hz, 1H), 8.22-8.17 (m, 1H), 8.00 (dd, J_1 = 8.4 Hz, J_2 = 1.8 Hz, 1H), 7.68 (s, 1H), 7.65-7.59 (m, 4H), 7.57-7.53 (m, 2H), 7.52-7.39 (m, 4H), 7.36-7.31 (m, 1H), 7.26 (d, J = 0.4 Hz, 1H), 7.24 (d, J = 0.8 Hz, 1H), 2.4 (s, 3H). ^{13}C NMR ($CDCl_3$, 400 MHz) δ (ppm) 142.23, 141.81, 141.53, 136.68, 137.02, 132.31, 130.00, 129.67, 127.93, 127.41, 127.01, 126.64, 126.02, 125.63, 123.73, 123.15, 122.03, 120.72, 120.65, 119.04, 110.15, 108.13, 21.19. MS (ESI) *m/z* 385.5 $[M+H]^+$, HRMS (MALDI-TOF): *m/z* 384.1610 [M^+, calcd 384.1621].

(Z)-2-(4-chlorophenyl)-3-(9-phenyl-9H-carbazol-3-yl)acrylonitrile (2e): Compound 2e was obtained from 2-(4-chlorophenyl)acetonitrile and 1. Time: 10 h Yield: 90%; pale green crystals; m.p. 228.3-228.6 °C; ^{1}H NMR ($CDCl_3$, 400 MHz): δ (ppm) 8.70 (d, J = 1.6 Hz, 1H) 8.19 (dd, J_1 = 8.0 Hz, J_2 = 0.8 Hz, 1H), 7.99 (dd, J_1 = 8.8 Hz, J_2 = 2 Hz, 1H), 7.67 (s, 1H), 7.66-7.58 (m, 4H), 7.57-7.38 (m, 8H), 7.36-7.31 (m, 1H). ^{13}C NMR ($CDCl_3$, 400 MHz) δ (ppm) 143.44, 142.14, 141.67, 136.99, 134.51, 133.75, 129.99, 129.14, 128.00, 127.51, 127.03, 126.96, 126.75, 125.62, 123.84, 123.12, 122.24, 120.83, 120.61, 118.54, 110.22, 110.20, 106.96. MS (ESI) *m/z* 405.5 $[M+H]^+$, HRMS (MALDI-TOF): *m/z* 404.1064 [M^+, calcd 404.1075].

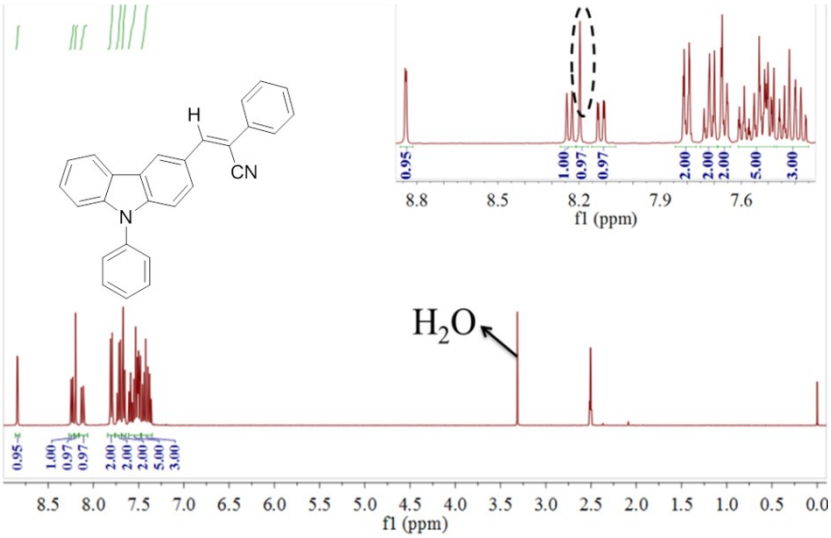

Fig. S1. ^{1}H NMR spectra of 2a.

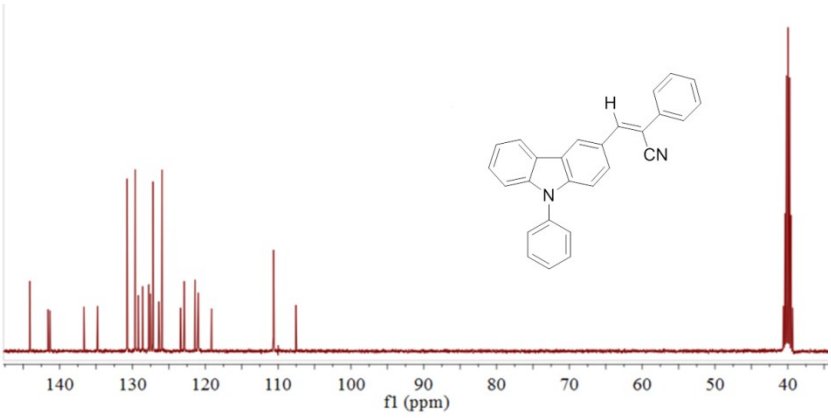

Fig. S2. ^{13}C NMR spectra of 2a.

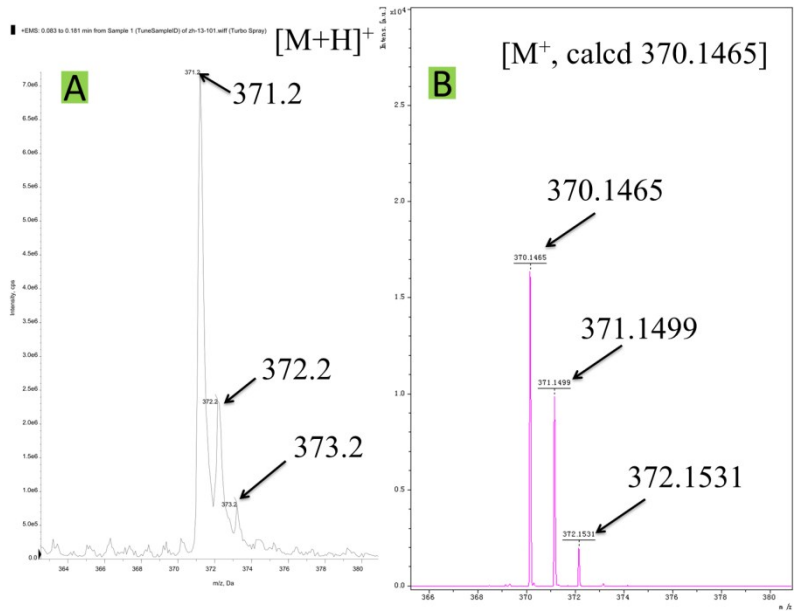

Fig. S3. (A) LRMS and (B) HRMS spectra of 2a.

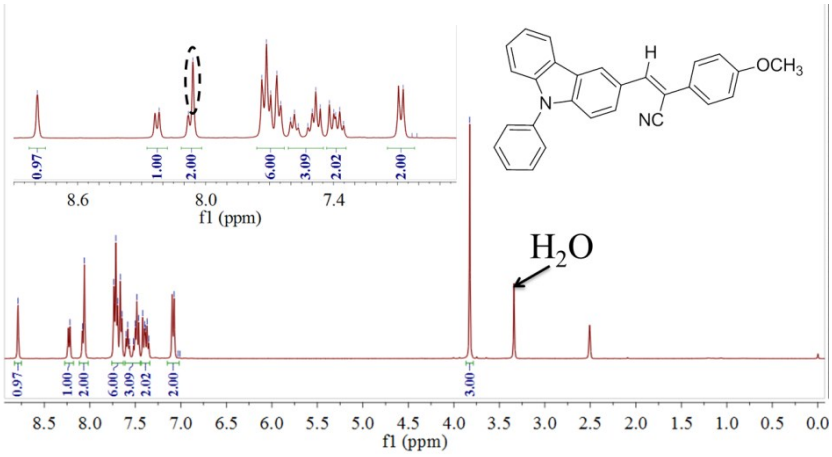

Fig. S4. ^{1}H NMR spectra of 2b.

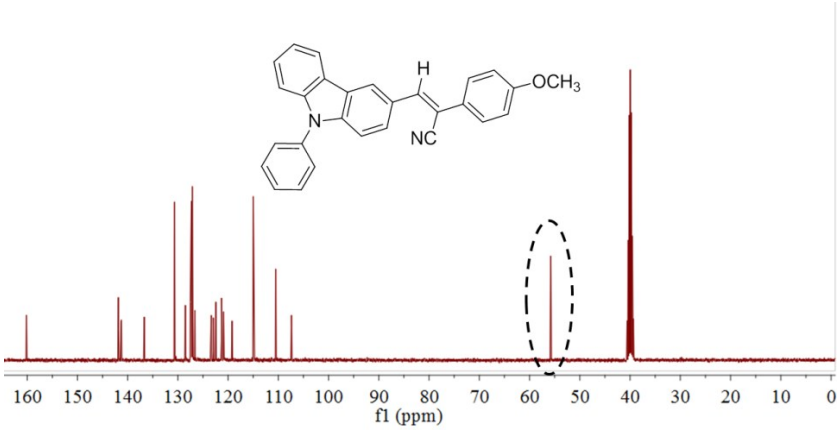

Fig. S5. ^{13}C NMR spectra of 2b.

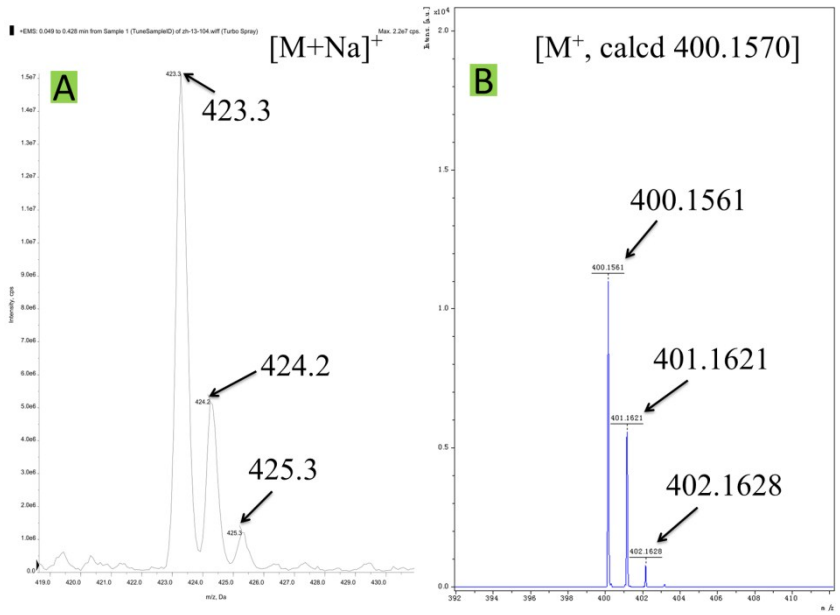

Fig. S6. (A) LRMS and (B) HRMS spectra of 2b.

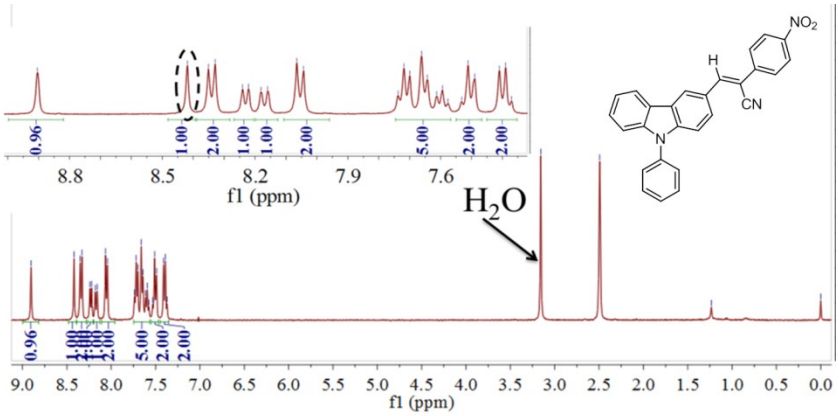

Fig. S7. ^{1}H NMR spectra of 2c.

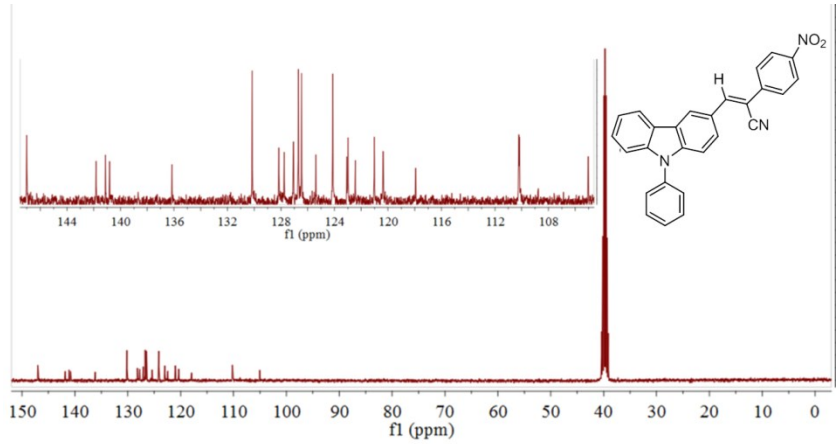

Fig. S8. ^{13}C NMR spectra of 2c.

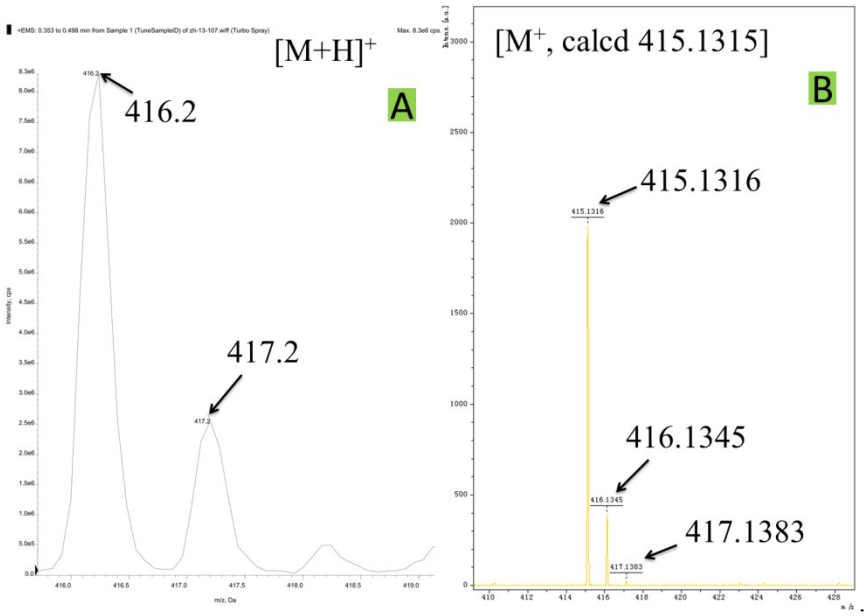

Fig. S9. (A) LRMS and (B) HRMS spectra of 2c.

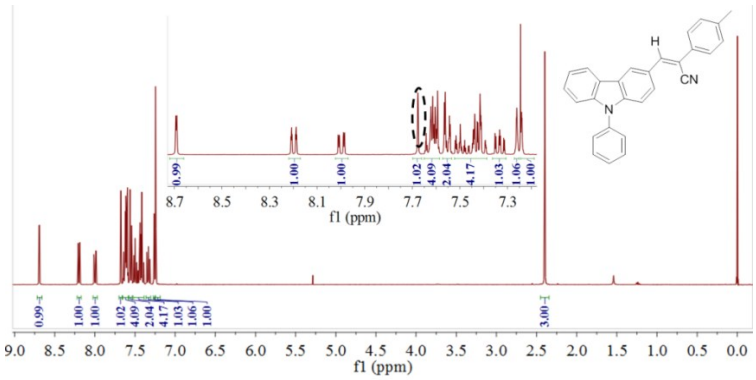

Fig. S10. ^{1}H NMR spectra of 2d.

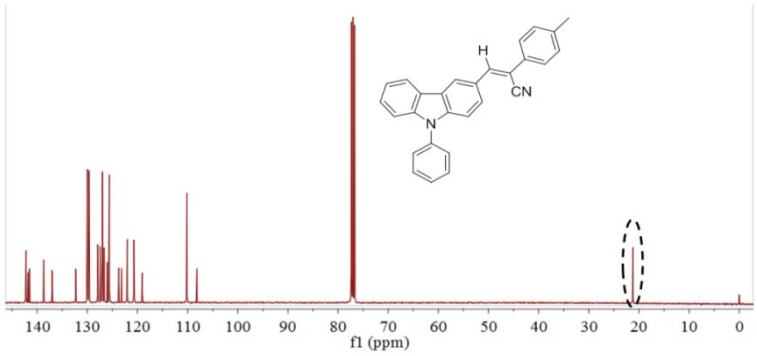

Fig. S11. ^{13}C NMR spectra of 2d.

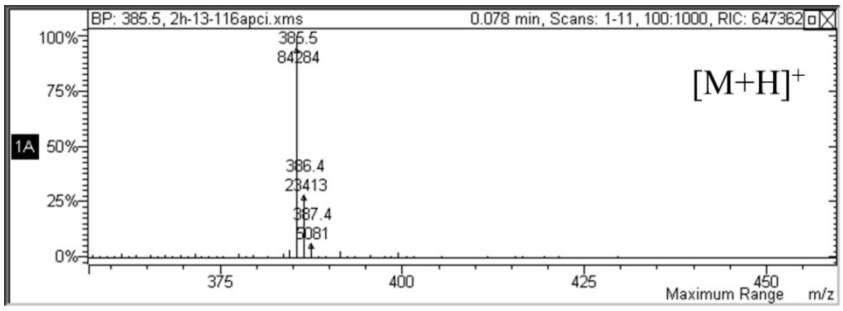

Fig. S12. LRMS spectra of 2d.

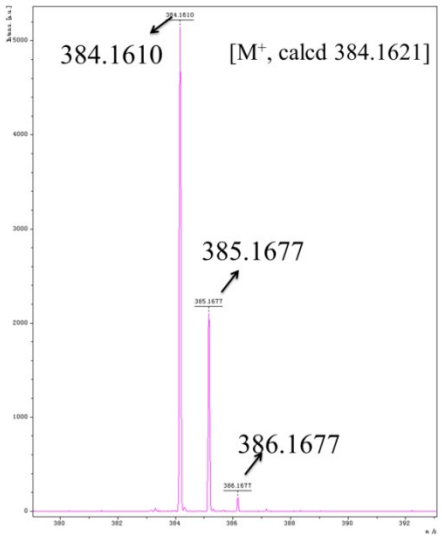

Fig. S13. HRMS spectra of 2d.

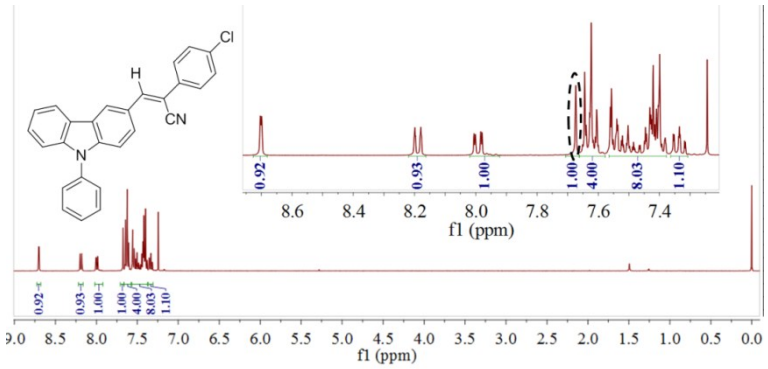

Fig. S14. ^{1}H NMR spectra of 2e.

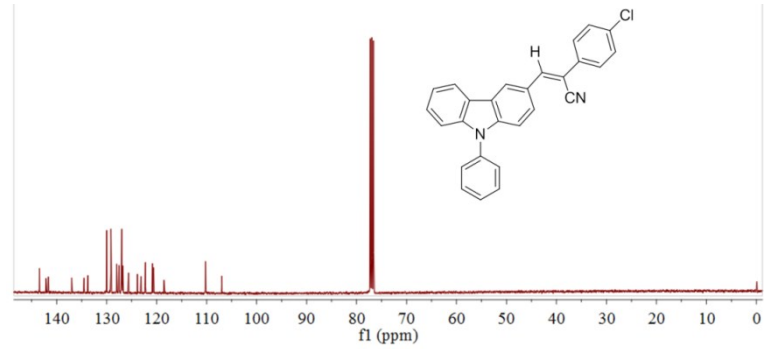

Fig. S15. ^{13}C NMR spectra of 2e.

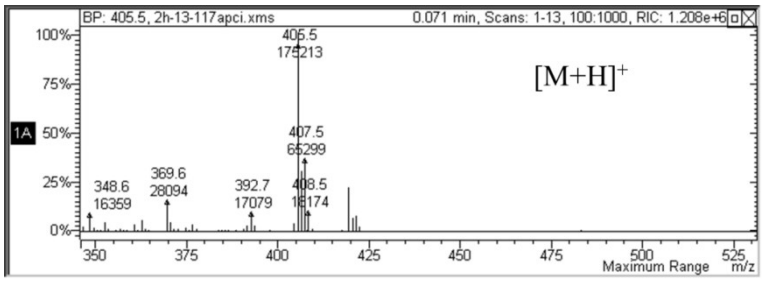

Fig. S16. LRMS spectra of 2e.

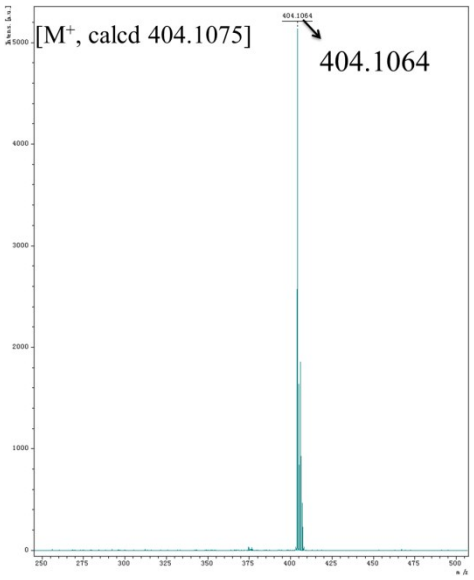

Fig. S17. HRMS spectra of 2e.

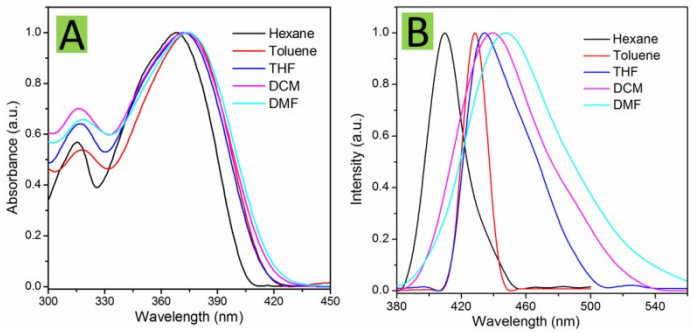

Fig. S18. Normalised (A) absorption and (B) emission spectra of 2a in various organic solvents.

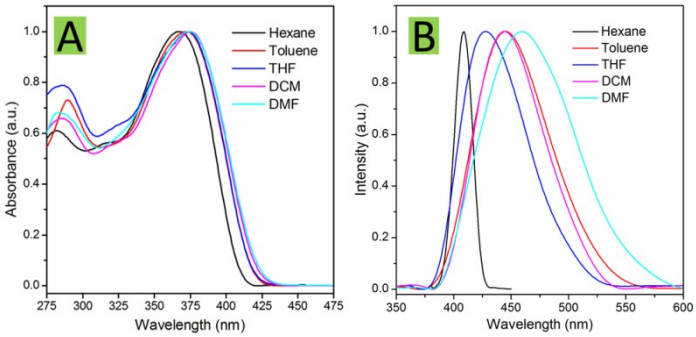

Fig. S19. Normalised (A) absorption and (B) emission spectra of 2b in various organic solvents.

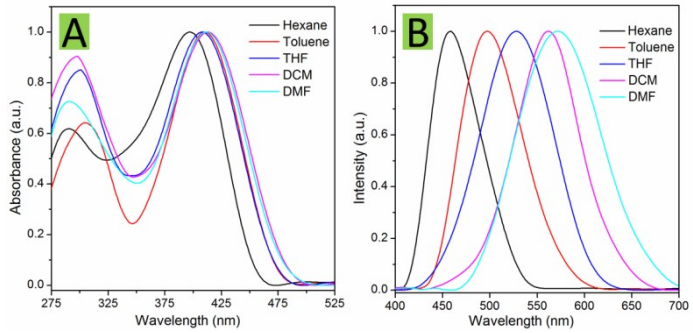

Fig. S20. Normalised (A) absorption and (B) emission spectra of 2c in various organic solvents.

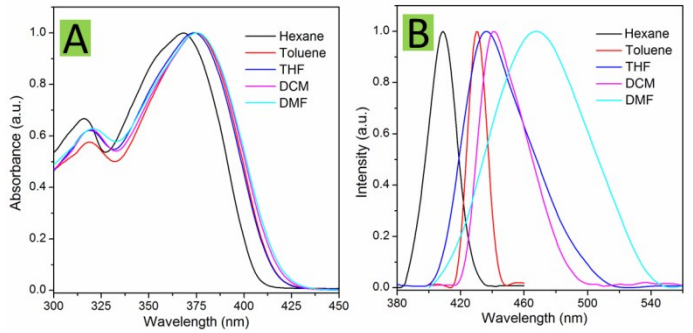

Fig. S21. Normalised (A) absorption and (B) emission spectra of 2d in various organic solvents.

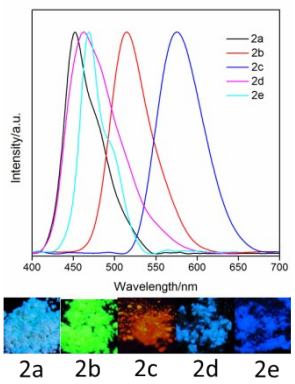

Fig. S22. Fluorescent emission spectra of the as-prepared 2a-2e and photographs of the powder of the as-prepared 2a-2e under 365 nm UV light.

Table S1 Photophysical properties of 2a-2e.

Compound	λ_{abs}[a] (nm)	λ_{em}[a] (nm)	Stokes shift (nm)	λ_{em}[b] (nm)	E_g[c] (eV)
2a	316, 372	439	67	452, 507[d]	3.11
2b	286, 375	444	69	515	3.08
2c	298, 413	562	149	575	2.76
2d	320, 375	441	66	462, 581[d]	3.10
2e	321, 380	451	71	469, 579[d]	3.05

[a]Measured in DCM. [b]Tested in solid state. [c]The optical band gap estimated from the onset wavelength of the absorption spectra in DCM. [d]The maximum emission wavelength of ground sample.

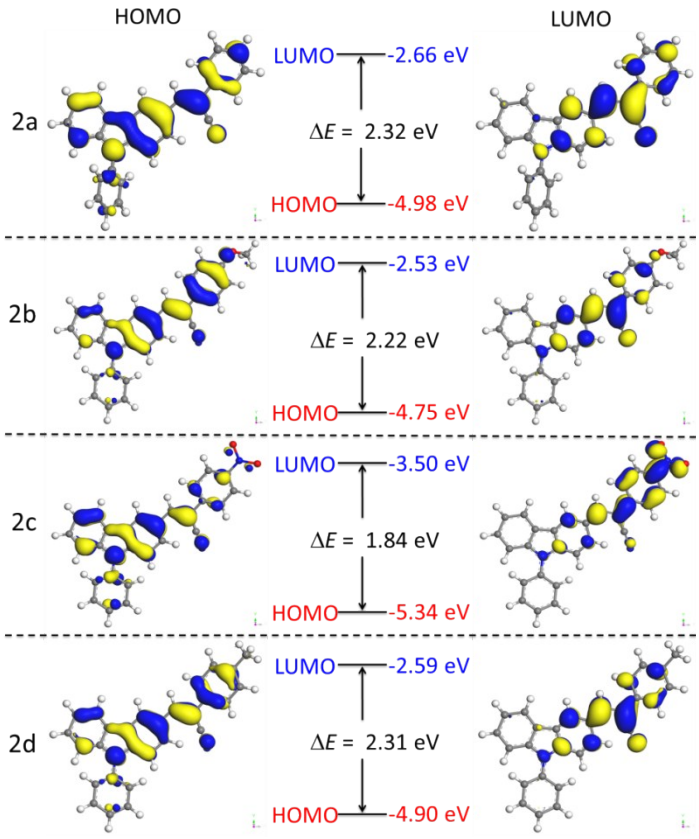

Fig. S23. B3LYP/6-31G(d) calculated molecular orbital amplitude plots of HOMO and LUMO levels for 2a-2d.

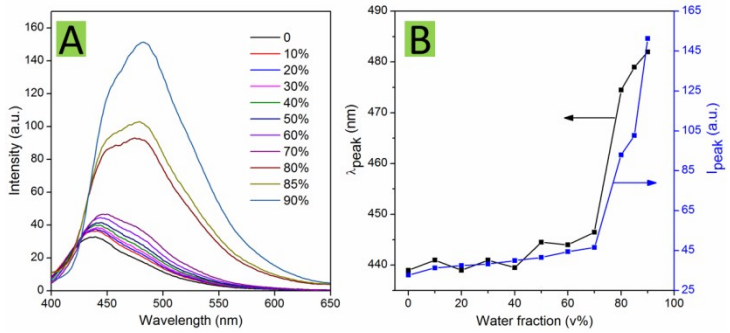

Fig. S24. (A) Emission spectra of 2a in THF and THF/water mixtures with varying water fractions (f_w). (B) Plots of fluorescence peak location and intensity *vs* f_w for 2a. Concentration = 20 μM; excitation wavelength = 360 nm.

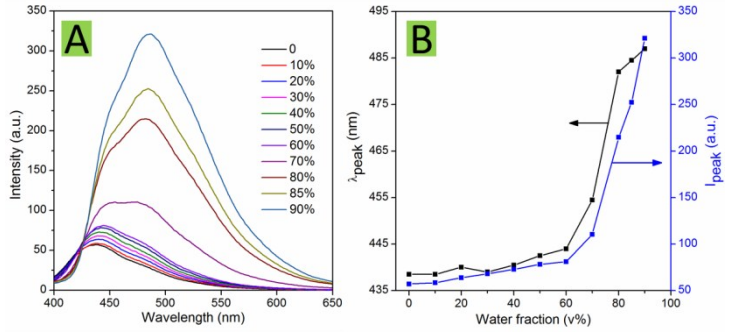

Fig. S25. (A) Emission spectra of 2b in THF and THF/water mixtures with varying water fractions (f_w). (B) Plots of fluorescence peak location and intensity *vs* f_w for 2b. Concentration = 20 μM; excitation wavelength = 360 nm.

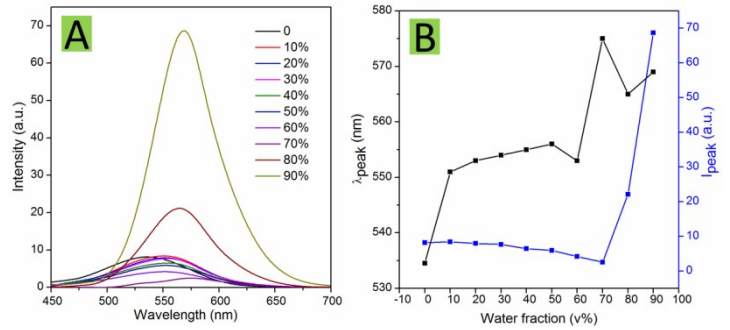

Fig. S26. (A) Emission spectra of 2c in THF and THF/water mixtures with varying water fractions (f_w). (B) Plots of fluorescence peak location and intensity *vs* f_w for 2c. Concentration = 20 μM; excitation wavelength = 360 nm.

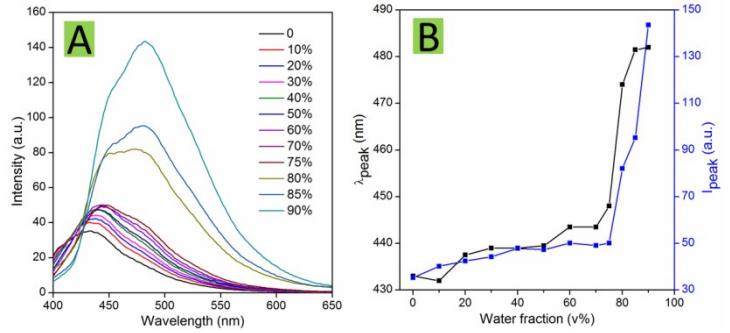

Fig. S27. (A) Emission spectra of 2d in THF and THF/water mixtures with varying water fractions (f_w). (B) Plots of fluorescence peak location and intensity *vs* f_w for 2d. Concentration = 20 μM; excitation wavelength = 360 nm.

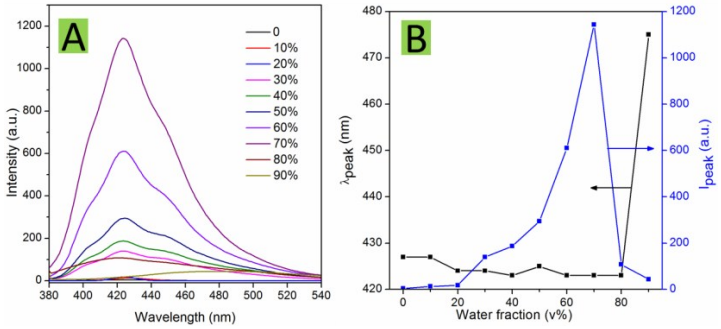

Fig. S28. (A) Emission spectra of 2a in THF and THF/water mixtures with varying water fractions (f_w) and kept at room temperature above 2 h. (B) Plots of fluorescence peak location and intensity *vs* f_w for 2a. Concentration = 20 μM; excitation wavelength = 360 nm.

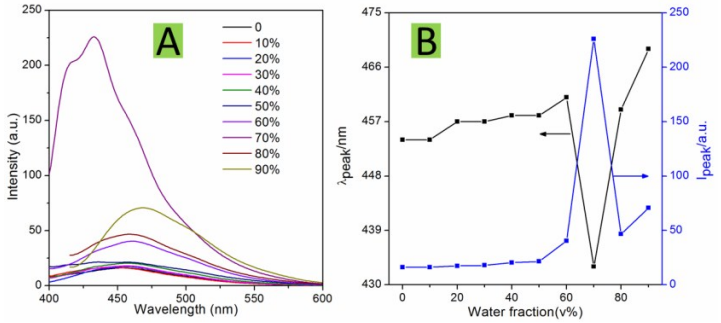

Fig. S29. (A) Emission spectra of 2b in THF and THF/water mixtures with varying water fractions (f_w) and kept at room temperature above 2 h. (B) Plots of fluorescence peak location and intensity *vs* f_w for 2b. Concentration = 20 μM; excitation wavelength = 360 nm.

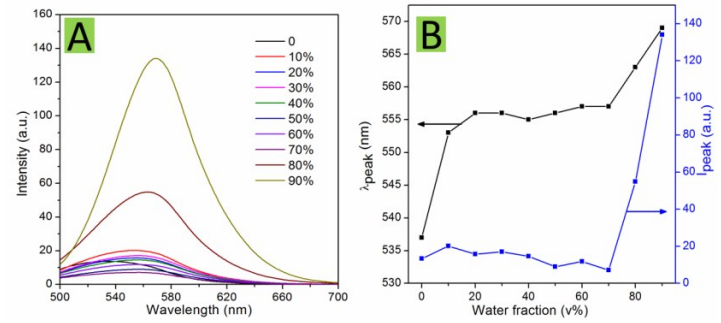

Fig. S30. (A) Emission spectra of 2c in THF and THF/water mixtures with varying water fractions (f_w) and kept at room temperature above 2 h. (B) Plots of fluorescence peak location and intensity *vs* f_w for 2c. Concentration = 20 μM; excitation wavelength = 360 nm.

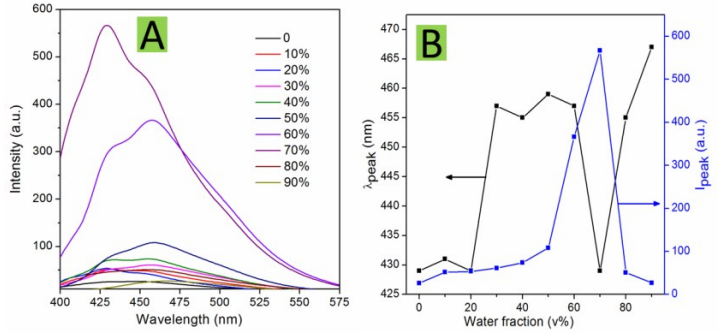

Fig. S31. (A) Emission spectra of 2d in THF and THF/water mixtures with varying water fractions (f_w) and kept at room temperature above 2 h. (B) Plots of fluorescence peak location and intensity *vs* f_w for 2d. Concentration = 20 μM; excitation wavelength = 360 nm.

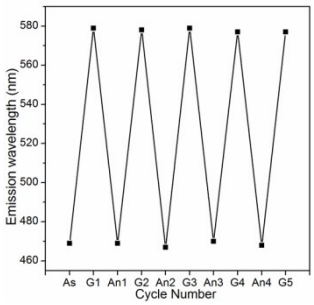

Fig. S32. Emission maxima of 2e during the grinding-annealing cycles. As = as prepared sample, G = ground sample; An= Annealing sample (annealing at 60 ^{o}C for 10 min). The numbers after G or An represent cycle numbers.

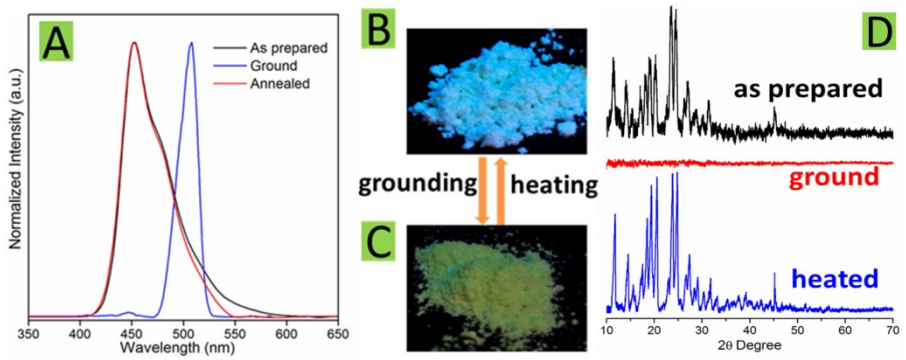

Fig. S33. (A) Emission spectra of the as prepared, ground and annealing 2a solids, (D) their XRD patterns and (B and C) their photographs taken under UV illumination.

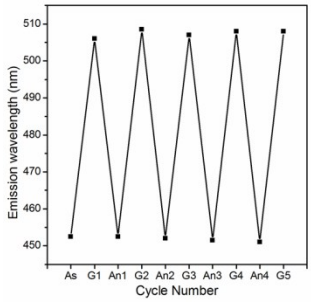

Fig. S34. Emission maxima of 2a during the grinding-annealing cycles. As = as prepared sample, G = ground sample; An= Annealing sample (annealing at 60 ^{o}C for 10 min). The numbers after G or An represent cycle numbers.

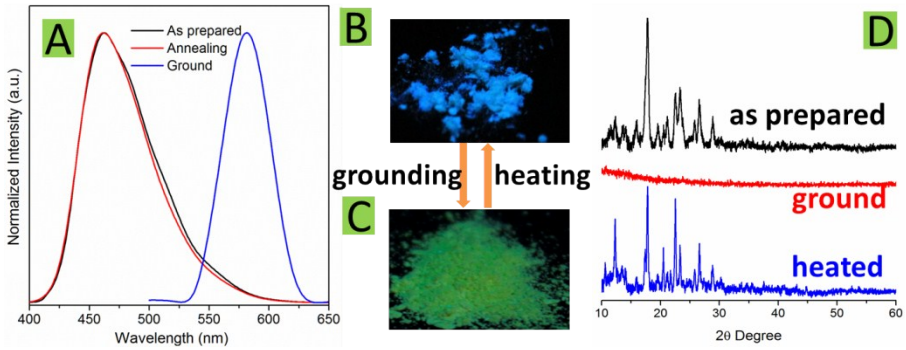

Fig. S35. (A) Emission spectra of the as prepared, ground and annealing 2d solids, (D) their XRD patterns and (B and C) their photographs taken under UV illumination.

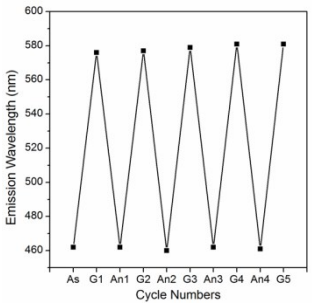

Fig. S36. Emission maxima of 2d during the grinding-annealing cycles. As = as prepared sample, G = ground sample; An= Annealing sample (annealing at 60 ^{o}C for 10 min). The numbers after G or An represent cycle numbers.

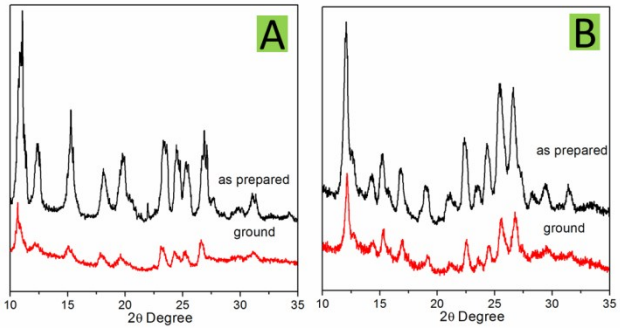

Fig. S37. XRD patterns of the as prepared and ground 2b (A) and 2c (B) solids.

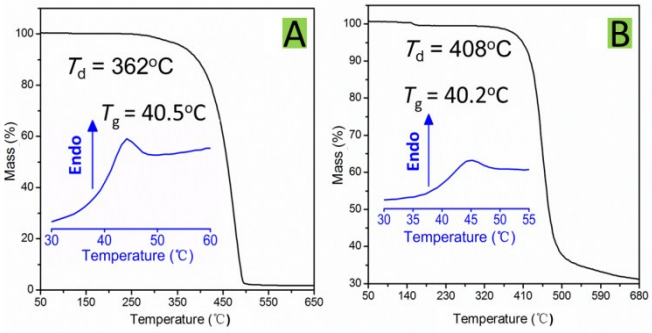

Fig. S38. TGA and DSC (inset) thermograms of 2a (A) and 2b (B) recorded under nitrogen atmosphere at the heating rate of 10 ^{o}C min^{-1}.

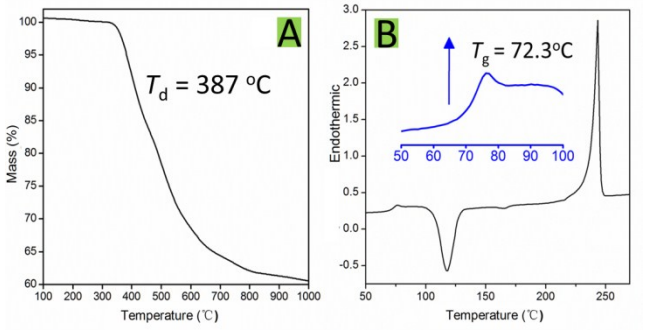

Fig. S39. (A) TGA thermograms of 2c recorded under nitrogen atmosphere at 10 °C min^{-1} scan rates. (B) DSC curve of the as-prepared 2c.

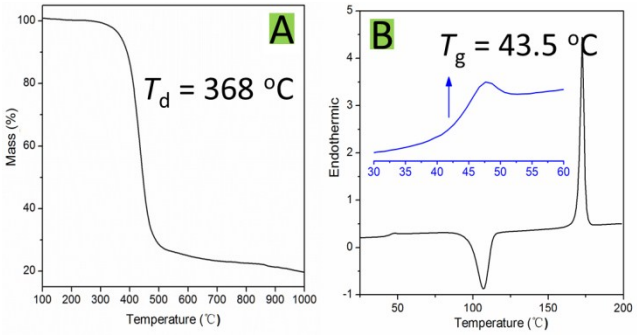

Fig. S40. (A) TGA thermograms of 2d recorded under nitrogen atmosphere at 10 °C min^{-1} scan rates. (B) DSC curve of the as-prepared 2d.

Table S2 Crystal data and structure refinement for 2a.

Identification code	2a	
Empirical formula	C27 H18 N2	
Formula weight	370.43	
Temperature	296.15 K	
Wavelength	0.71073 Å	
Crystal system	Monoclinic	
Space group	P 1 21/c 1	
Unit cell dimensions	a = 18.495(4) Å	α= 90°
	b = 13.396(3) Å	β= 96.436(4)°
	c = 7.8586(17) Å	γ = 90°
Volume	1934.7(7) $Å^3$	
Z	4	
Density (calculated)	1.272 Mg/m^3	
Absorption coefficient	0.075 mm^{-1}	
F(000)	776	
Crystal size	0.23 x 0.21 x 0.2 mm^3	
Theta range for data collection	1.108 to 25.063°	
Index ranges	-21<=h<=21, -15<=k<=15, -8<=l<=9	
Reflections collected	11027	
Independent reflections	3374 [R(int) = 0.0624]	
Completeness to theta = 25.063°	98.3 %	
Absorption correction	Semi-empirical from equivalents	
Max. and min. transmission	0.9852 and 0.9830	
Refinement method	Full-matrix least-squares on F^2	
Data / restraints / parameters	3374 / 0 / 263	
Goodness-of-fit on F^2	1.019	
Final R indices [I>2sigma(I)]	R1 = 0.0506, wR2 = 0.1193	
R indices (all data)	R1 = 0.0839, wR2 = 0.1412	
Extinction coefficient	0.017(2)	
Largest diff. peak and hole	0.215 and -0.223 $e.Å^{-3}$	

Table S3. Crystal data and structure refinement for 2b.

Identification code	2b	
Empirical formula	C28 H20 N2 O	
Formula weight	400.46	
Temperature	296.15 K	
Wavelength	0.71073 Å	
Crystal system	Monoclinic	
Space group	P 1 21/n 1	
Unit cell dimensions	a = 16.599(4) Å	α= 90°
	b = 7.731(2) Å	β= 111.991(4)°
	c = 17.121(4) Å	γ = 90°
Volume	2037.1(9) $Å^3$	
Z	4	
Density (calculated)	1.306 Mg/m^3	
Absorption coefficient	0.080 mm^{-1}	
F(000)	840	
Crystal size	0.21 x 0.2 x 0.19 mm^3	
Theta range for data collection	1.458 to 25.003°	
Index ranges	-19<=h<=19, -8<=k<=9, -20<=l<=19	
Reflections collected	9995	
Independent reflections	3591 [R(int) = 0.0360]	
Completeness to theta = 25.003°	99.9 %	
Absorption correction	Semi-empirical from equivalents	
Max. and min. transmission	0.9850 and 0.9834	
Refinement method	Full-matrix least-squares on F^2	
Data / restraints / parameters	3591 / 0 / 280	
Goodness-of-fit on F^2	1.021	
Final R indices [I>2sigma(I)]	R1 = 0.0425, wR2 = 0.1016	
R indices (all data)	R1 = 0.0695, wR2 = 0.1188	
Extinction coefficient	n/a	
Largest diff. peak and hole	0.146 and -0.204 $e.Å^{-3}$	

Table S4. Crystal data and structure refinement for 2c.

Identification code	2c	
Empirical formula	C27 H17 N3 O2	
Formula weight	415.43	
Temperature	296.15 K	
Wavelength	0.71073 Å	
Crystal system	Monoclinic	
Space group	P 1 21/c 1	
Unit cell dimensions	a = 17.245 (11) Å	α= 90°
	b = 13.979(9) Å	β= 103.290(10)°
	c = 8.714(6) Å	γ = 90°
Volume	2044(2) $Å^3$	
Z	4	
Density (calculated)	1.350 Mg/m^3	
Absorption coefficient	0.087 mm^{-1}	
F(000)	864	
Crystal size	0.21 x 0.2 x 0.19 mm^3	
Theta range for data collection	2.809 to 25.027°	
Index ranges	-19<=h<=20, -16<=k<=14, -9<=l<=10	
Reflections collected	10081	
Independent reflections	3600 [R(int) = 0.1002]	
Completeness to theta = 25.027°	99.5 %	
Refinement method	Full-matrix least-squares on F^2	
Data / restraints / parameters	3600 / 0 / 290	
Goodness-of-fit on F^2	0.977	
Final R indices [I>2sigma(I)]	R1 = 0.0840, wR2 = 0.1974	
R indices (all data)	R1 = 0.1883, wR2 = 0.2614	
Extinction coefficient	0.016(4)	
Largest diff. peak and hole	0.328 and -0.262 $e.Å^{-3}$	

Table S5. Crystal data and structure refinement for 2d.

Identification code	2d	
Empirical formula	C28 H20 N2	
Formula weight	384.46	
Temperature	296.15 K	
Wavelength	0.71073 Å	
Crystal system	Monoclinic	
Space group	P 1 21/c 1	
Unit cell dimensions	a = 16.517(4) Å	α= 90°
	b = 13.934(3) Å	β= 103.642(4)°
	c = 9.048(2) Å	γ = 90°
Volume	2023.7(8) $Å^3$	
Z	4	
Density (calculated)	1.262 Mg/m^3	
Absorption coefficient	0.074 mm^{-1}	
F(000)	808	
Crystal size	0.27 x 0.25 x 0.22 mm^3	
Theta range for data collection	1.269 to 25.192°	
Index ranges	-19<=h<=19, -16<=k<=16, -10<=l<=8	
Reflections collected	11762	
Independent reflections	3637 [R(int) = 0.0602]	
Completeness to theta = 25.192°	99.9 %	
Absorption correction	Semi-empirical from equivalents	
Max. and min. transmission	0.9839 and 0.9803	
Refinement method	Full-matrix least-squares on F^2	
Data / restraints / parameters	3637 / 0 / 273	
Goodness-of-fit on F^2	0.954	
Final R indices [I>2sigma(I)]	R1 = 0.0516, wR2 = 0.1164	
R indices (all data)	R1 = 0.1029, wR2 = 0.1429	
Extinction coefficient	0.0096(14)	
Largest diff. peak and hole	0.213 and -0.149 $e.Å^{-3}$	

Table S6. Crystal data and structure refinement for 2e.

Identification code	2e	
Empirical formula	C27 H17 Cl N2	
Formula weight	404.88	
Temperature	296.15 K	
Wavelength	0.71073 Å	
Crystal system	Monoclinic	
Space group	P 1 21/c 1	
Unit cell dimensions	a = 16.672(12) Å	α= 90°
	b = 13.929(10) Å	β= 102.965(8)°
	c = 8.865(6) Å	γ = 90°
Volume	2006(2) $Å^3$	
Z	4	
Density (calculated)	1.340 Mg/m^3	
Absorption coefficient	0.207 mm^{-1}	
F(000)	840	
Crystal size	0.21 x 0.2 x 0.19 mm^3	
Theta range for data collection	1.926 to 25.008°	
Index ranges	-19<=h<=19, -16<=k<=16, -10<=l<=10	
Reflections collected	15755	
Independent reflections	3546 [R(int) = 0.0273]	
Completeness to theta = 25.008°	100.0 %	
Absorption correction	Semi-empirical from equivalents	
Refinement method	Full-matrix least-squares on F^2	
Data / restraints / parameters	3546 / 0 / 271	
Goodness-of-fit on F^2	1.132	
Final R indices [I>2sigma(I)]	R1 = 0.0388, wR2 = 0.1068	
R indices (all data)	R1 = 0.0541, wR2 = 0.1262	
Extinction coefficient	n/a	
Largest diff. peak and hole	0.169 and -0.266 $e.Å^{-3}$	

References

1. R. Lygaitis, J. V. Grazulevicius and V. Jankauskas, *Mol Cryst Liq Cryst*, 2011, **536**, 182/[414]-191/[423].
2. Y. Zhang, G. Zhuang, M. Ouyang, B. Hu, Q. Song, J. Sun, C. Zhang, C. Gu, Y. Xu and Y. Ma, *Dyes Pigments*, 2013, **98**, 486-492.
3. S. S. Kulp and C. B. Caldwell, *The Journal of Organic Chemistry*, 1980, **45**, 171-173.